Experimental report

30/05/2022

Proposal: **1-05-18**

Council: 4/2020

Title: 4D coupled hydromechanics of porous rocks

Research area: Other...

This proposal is a new proposal

Main proposer: **Stephen HALL**

Experimental team: Jonas ENGQVIST
Fernando LIMA
Robin WORACEK
Stephen HALL
Erika TUDISCO

Local contacts: Alessandro TENGATTINI

Samples: synthetic rock

Instrument	Requested days	Allocated days	From	To
NEXT	5	4	09/06/2021	13/06/2021

Abstract:

Heterogeneity due to localised deformation has significant effects on rock permeability, giving rise to anisotropic flow and producing barriers or conduits. Understanding these effect is key to optimising processes involving extraction or injection of fluids in geologic reservoirs, e.g., hydrocarbon and water production or CO2 sequestration, and understanding natural processes, e.g., earthquake mechanisms. We will perform coupled hydro-mechanical in-situ experiments with 3D imaging of both the evolution of sample structure and of the pressure-driven flow of H2O into D2O saturated samples. The resultant image data will be high-resolution tomographies recording structural evolution, which will be analysed by DVC to quantify the strain field evolution, plus 4D images tracking the fluid flow field at each deformation state. The latter will be analysed to determine the flow velocity field and compared with the strain field evolution to provide the first such data on the coupling of deformation and changes in fluid flow. Different deformation mechanisms will be explored by testing at different confining pressure, from dilatant shear failure to compaction bands.

ILL EXPERIMENTAL REPORT

The experiments were performed from the 9th to the 13th of June of 2021 using the NeXT instrument at the Institut Laue-Langevin. The campaign's objective was to acquire x-ray and neutron tomography data during in-situ, coupled hydromechanical triaxial tests to better understand the micro-scale hydromechanical couplings in porous rock (in this case, Idaho Gray Sandstone) and their connection to macroscopic observations obtained at the sample boundaries.
An experimental setup consisting of 4 subsystems was installed in the instrument to carry out the tests. It comprises the portable load system, the confining pressure system, the fluid flow system and the triaxial cell (see schematic in Figure 1). Figure 2 depicts the assembly of the compression device, flow and confining pressure systems at NEXT.

For the neutron imaging, the distance between the experimental cell and the detector was the minimum possible (around 5 mm) to minimize image blur, whilst still permitting rotation of the system for tomography. Th rotation was achieved using a rotation system integrated within the external loading frame permitting rotation under axial load. For x-ray tomography, the same approach was initially adopted. Unfortunately, the combination of imprecision in the axis of rotation of the loading device and the cone-beam resulted in poor quality images. Thus, it was decided to rotate the entire compression device, increasing the distance between the cell and the detector (to 150 mm). This resulted in shadowing of images at some angles due to obstruction by the device's frame, but better-quality images were obtained.

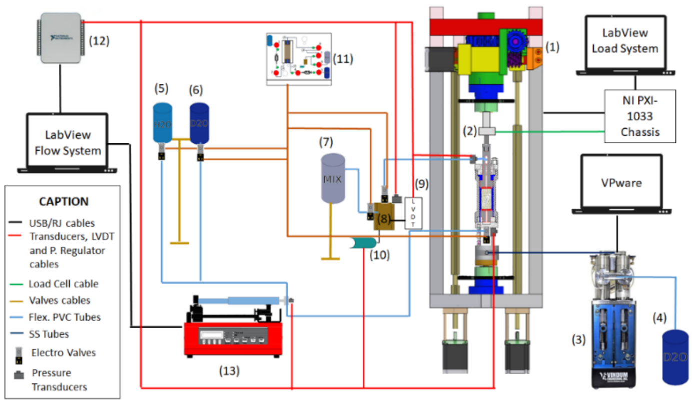

Figure 1 - The schematic diagram of the experimental setup: (1) Load Device; (2)Load Cell; (3)Vindum Pump VP-12; (4)Heavy water pressure system reservoir; (5)Normal water flow system reservoir; (6)Heavy water flow system reservoir; (7)Mixed flow system reservoir; (8) Air-water Interface; (9)LVDT; (10) Pressure Regulator; (11) Valve Control Box; (12)National Instruments ADC interface; (13)Double-syringe Pump.

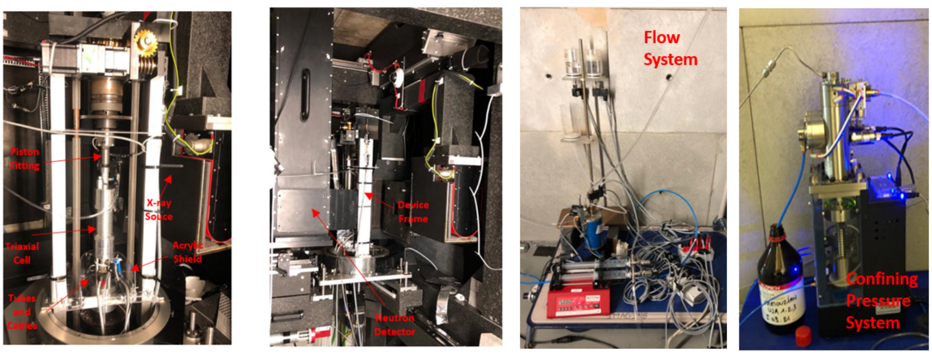

Figure 2 - Testing system mounted on NeXT, ILL facility. (a) Compression Device and Triaxial Cell; (b) Compression Device in neutron tomography position; (c) Flow System; (d) Confining Pressure System

One flow test and two coupled hydro-mechanical tests were performed. For all tests, the initial procedures were according to the following. After the system setup, a confinement pressure of 1 MPa was applied to the sample inside the cell and the sample, which was withi a Viton® membrane, was saturated with heavy water. Initially, it was intended to apply 5 MPa in the second sample. However, the attempt was frustrated by technical problems with the membrane. After stabilizing the confining pressure, the first high-resolution neutron tomography acquisition was performed, involving 1250 radiographic projections acquired during rotation of the sample over 180° at 0,1°/s with an exposure time of 1.5 s and 43 µm pixel size. The total tomography scan time was 30 minutes. Next, an x-ray tomography scan was performed by rotating the whole device over 360°, using the beamline rotation stage and using a tube voltage of 140 kV and a current of 200 mA. Each scan comprised 1200 radiographic projections, with 1.4 s exposure time and a total time of 30 minutes. The voxel size in the reconstructed tomography images was 55 µm for all samples

Once the high-resolution x-ray and neutron scans were completed, the first flow test was started. H_2O was pushed into the bottom of the D_2O saturated sample under rate-control using the syringe pump. During the H_2O injection high-speed neutron tomographies were performed with 700 radiographic projections during 180° rotation of the sample at a velocity of 3°/s (170 µm pixel size and 0.09 s exposure), resulting in a 1-minute duration for each tomography. The nominal H_2O flow rate was 0.07 ml/min, chosen based on an assumption that the theoretical advance of the infiltration front could be identified by the high-speed tomography with a maximum displacement of 1 pixel during a 180° scan. The fluid pressure was measured at the top and bottom of the cell, allowing the pressure drop determination during percolation, from which a permeability calculation was made based on the premise of a constant flow rate. The criterion to end the flow tests was that the outlet grayscale intensity reached the same values as the inlet (indicating full saturation). Each flow experiment lasted for about 1.0-2.5 hrs. The axial compression of each step was performed at a constant displacement rate of 1 µm/s (strain rate = $2 \times 10{-}5$ s^{-1}), as in (47) until a pre-defined deformation. The axial force was recorded using the load cell, the axial displacement was assumed based on the prescribed compression rate and the Vindum Pump measured the volumetric displacement. Data from the compression device and the pump were saved every second. One high-resolution neutron tomography was performed after every deformation. After each high-resolution tomography a flow test was initialized. These cycles were repeated until sample failure (the loading was stopped immediately post-peak). Finally, an x-ray tomography was carried out after the loading was stopped. Figure 3 shows a the stress-strain curved for the deviatoric compression of sample 1 highlighting the imaging performed at the different stages of the test.

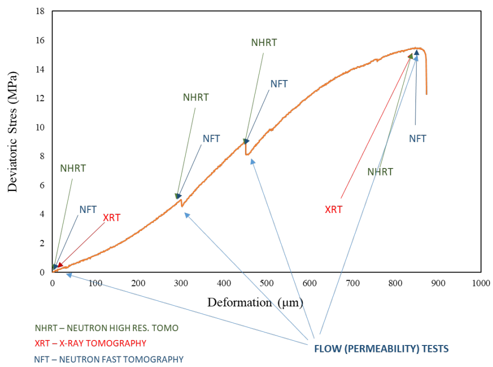

Fig. 3 - Sample 1 compression and imaging times.

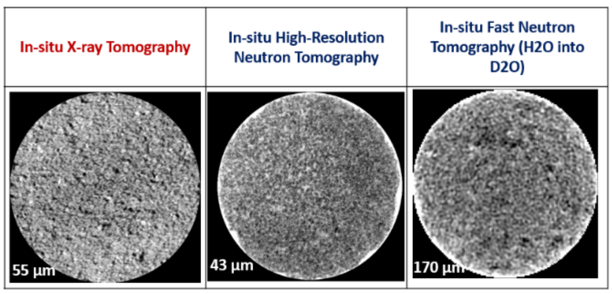

Fig. 4 - Cross-sections of tomography images

In summary, the imaging data acquired for the three samples comprises 13 high-resolution neutron tomographies, 6 x-ray tomographies, 11 fast neutron tomographies (multi-tomo), and 15 radiographies to monitor and the sample and equipment during the test. Reconstruction of the spatial information on the linear attenuation coefficient in the samples was done with the XAct software. Figure 4 shows some cross-sections of each type of tomography.

INITIAL RESULTS

Some initial results of the two coupled triaxial-flow tests are presented from the image data acquired during the experiments and the boundary measurements. The stress, porosity reduction and relative permeability variation with axial strain are shown in Figure 5 for both samples.

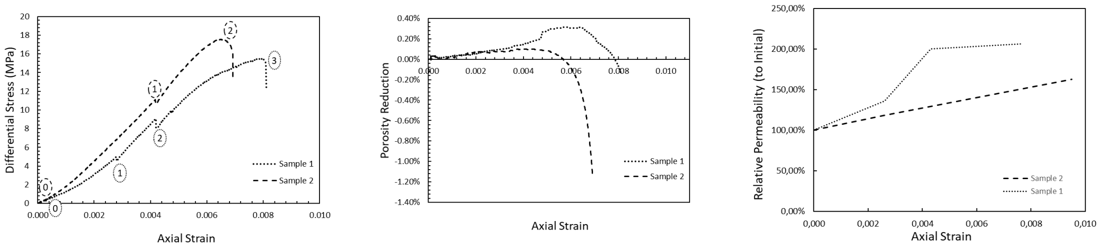

Figure 5 - Mechanical and hydraulic data

Python codes were developed to generate porosity maps of samples from the neutron and x-ray images. Indications of localized deformation can be noted in the porosity map slices presented in Figure 6, but this is much more apparent in the volumetric and shear strain fields obtained by Digital Volume Correlation (DVC) performed with the SPAM software on both the x-ray and neutron image data (Figure 7). Furthermore, the high-speed neutron multi-tomography results indicate preferential flow paths through the samples (see Figure 8). Voxel saturation time and z-speed fields were generated by applying an in-house Python code. The average speed measured from the images was 10x higher than expected, considering the flow rate and the total cross-section area, validating the hypothesis of the flow being confined to a preferential path that is narrower that the sample diameter (Figure 8).

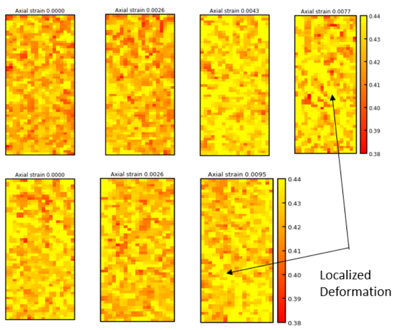

Figure 6 - Slices of the Porosity Maps

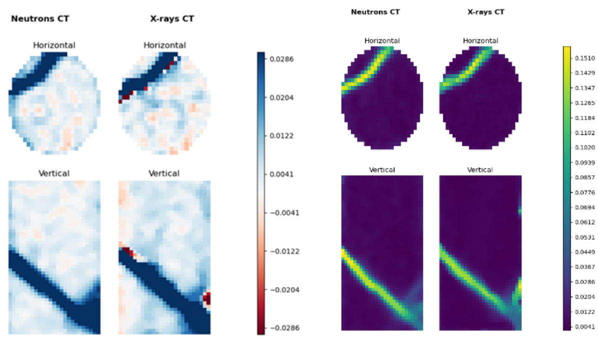

Figure 7 – Slices of (a) Volume and (b) Shear Strain Fields from Digital Volume Correlation

In future experiments, adopting a new axial compression system will allow the use of the NeXT rotation table and the reduction of the sample-detector distance, providing better resolution of the images. This upgrade will enable, for example, higher resolution x-ray images to be acquired at each loading stage that can be analysed interms of the granular structure. In addition, tests with different confining pressures will be perfomerf to investigate the influence of stress state on the hydromechanical behavior of the material. In the last experiment carried out in this campaign, radiographs obtained during application of the confining pressure allowed the cause of the membrane failures to be identified.

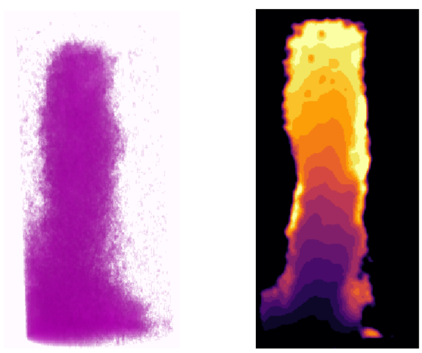

Figure 8 – (Left) Preferential flow visualized by transparency thresholding of the high-speed neutron tomography data acquired after percolation of the H_2O. (Right) Voxel saturation time (vertical slice through the volume) determined from the full set of high-speed neutron tomographies for Sample 1.